A Brain-Controlled Switch for Asynchronous Control Applications

S. G. Mason*, *Member, IEEE* and G. E. Birch, *Member, IEEE*

***Abstract*—Asynchronous control applications are an important class of application that has not received much attention from the brain-computer interface (BCI) community. This work provides a design for an asynchronous BCI switch and performs the first extensive evaluation of an asynchronous device in attentive, spontaneous electroencephalographic (EEG). The switch design [named the low-frequency asynchronous switch design (LF-ASD)] is based on a new feature set related to imaginary movements in the 1–4 Hz frequency range. This new feature set was identified from a unique analysis of EEG using a bi-scale wavelet. Offline evaluations of a prototype switch demonstrated hit (true positive) rates in the range of 38%–81% with corresponding false positive rates in the range of 0.3%–11.6%. The performance of the LF-ASD was contrasted with two other ASDs: one based on mu-power features and another based on the outlier processing method (OPM) algorithm. The minimum mean error rates for the LF-ASD were shown to be significantly lower than either of these other two switch designs.**

***Index Terms*—Asynchronous control, BCI, brain, computer, EEG, human, interface, machine, switch.**

NOMENCLATURE

ASD	Asynchronous switch design. A type of switch designed for asynchronous control applications.
IVMRP	Imagined voluntary movement-related potentials. Electroencephalographic (EEG) potentials related to imagined voluntary movement.
LF-ASD	The ASD proposed and evaluated in this paper. LF-ASD is an acronym for low-frequency asynchronous switch design.
LVQ3	A vector quantization method. For details, refer to [11].
Mu-ASD	An experimental ASD based on changes in mu-rhythm power.
OPM	Acronym for the outlier processing method. A method to extract and classify single-trial movement related potentials from EEG.
OPM-ASD	An experimental ASD based on the OPM algorithm.
$P(FP)$	Probability of a false positive. i.e., the probability of the ASD incorrectly classifying EEG when the user is idle as a switch activation.
$P(TP)$	Probability of a true positive. i.e., the probability of the ASD correctly classifying an attempted switch activation as a switch activation.
ROCC	Acronym for receiver operating characteristics curve. See description of ROCCs in Section IV.
VMRP	Voluntary movement-related potentials. EEG Potentials related to voluntary movement.

Manuscript received Novembaer 10, 1998; revised June 14, 2000. This work was supported by the Natural Sciences and Engineering Research Council of Canada under Grant 90278-96 and by the Government of British Columbia's Information, Science and Technology Agency. *Asterisk indicates corresponding author*.

*S. G. Mason is with the Neil Squire Foundation, 220–2250 Boundary Road, Burnaby, BC, V5M 4L9, Canada (e-mail: sgmason@ieee.org).

G. E. Birch is with the Neil Squire Foundation, the Department of Electrical and Computer Engineering, The University of British Columbia, Vancouver, BC, V6T 1Z4, Canada.

Publisher Item Identifier S 0018-9294(00)08518-9.

I. INTRODUCTION

AS A RESULT of accident or disease, millions of people worldwide suffer from a severe loss of motor function. These people are forced to accept a reduced quality of life dependent on other individuals. Technical aids have been developed to liberate these individuals, but the effectiveness of these aids for individuals with severe disabilities is often limited by the human-machine interface.

The concept of a brain-computer interface (BCI) has emerged over the last two decades of research as a promising alternative. The ultimate goal of this research has been to create an advanced communication interface that will allow an individual to control a device, such as a wheelchair or computer, with signals measured from the brain. This type of interface would increase an individual's independence, leading to an improved quality of life and reduced social costs. The majority of these techniques have focused on EEG data and these have shown that EEG activity may be a good basis for such communication and control channels.

In a typical BCI based on spontaneous EEG, the operator generates a "control signal" by consciously changing his cognitive state when he or she wants to control the device. The change in cognitive state is measured as specific temporal patterns [1], [2] signal power level [3]–[7] in the operator's EEG activity. Several techniques have been realized with varying degrees of success [8].

The design of a BCI depends on the application for which it was intended. To date most researchers have designed and tested BCI systems on, what we will call, synchronous control applications. In these applications, the system initiates a new control period when the operator has completed the previous control task or the system has timed out. The sequencing of actions in this type of application is illustrated in Fig. 1. Note, in these applications, the system initiates the period of control, not the user, and the user is expected to be consciously controlling the interface during the control periods.

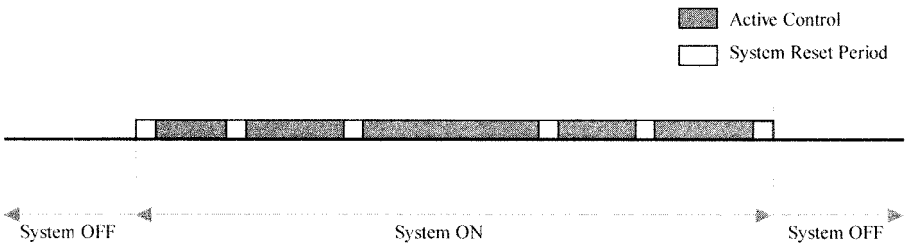

Fig. 1. Sequence of events for a synchronous control or communication application.

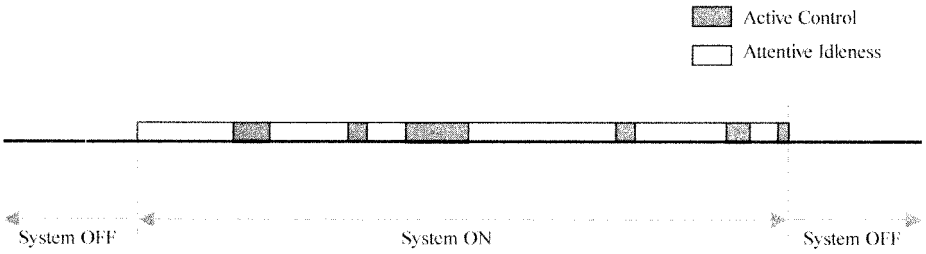

Fig. 2. Typical sequence of events in an asynchronous control application.

In contrast, there are applications that require constant user attention and irregular, user-initiated (not system-initiated) control. These types of application are usually not communications applications, but control applications. Monitoring a process and adjusting a control level when required is an example of this type of application. These types of applications, which we will call asynchronous control applications, are characterized by alternating periods of attentive idleness and active control as illustrated in Fig. 2. In these applications, the user is not consciously controlling their state when they are attentively idle. The user only consciously controls their state when they desire to control the device.

The asynchronous control application domain is an important class of applications that has received little attention from the BCI research community. This is partially because the application domains have lacked definition and partially because the field has lacked a mechanism to determine when EEG control is intended and when it is not.[1] Since the concept of asynchronous control is new to many readers, there may be some confusion regarding the differentiation of application domains and use of terminology. Also asynchronous control detection may be confused with the System On/Off Problem. To clarify the latter point, let us look at Figs. 1 and 2. We have drawn both these figures with System ON and System OFF periods to emphasize that the mechanism to detect asynchronous control signals from attentive, idle EEG is different from the mechanism to turn the system on. They are not the same mechanism: the asynchronous signal detector has to differentiate between attentive idle EEG and the control states, whereas the System ON mechanism is more complicated; it has to differentiate between all possible innate brain states and the system on state. In theory, the asynchronous control environment could be implemented with the sequence System ON, control commands, System OFF for every control command required. Practically, this theoretical implementation is burdensome to the user and adds additional delays in the control stream.

In this paper, we introduce the prototype of a BCI switch suitable for asynchronous control applications and evaluate its performance offline. The performance of this device is compared with the performance of two other asynchronous switches—one created using the outlier processing method (OPM) [1] as its basis and the other using a mu-rhythm power classification algorithm [3], [6] as its basis. This research is novel in two respects: it marks the first extensive evaluation of asynchronous signal detection device in attentive, spontaneous EEG; and the asynchronous switch is controlled by a new EEG feature basis related to an imagined finger movement. The introduction of our switch design, the low-frequency asynchronous switch design (LF-ASD), provides the first step toward a critical class of component for asynchronous control applications.

The remainder of the paper is organized in four sections. Section II presents the design of our asynchronous switch. Section III describes the methods used to evaluate the performance of proposed switch design and the performance of the two switches based on OPM and mu-event-related desynchronization (ERD). Section IV presents the results of our evaluation. Section V summarizes our findings and outlines our future research efforts. A glossary of abbreviations is provided at the beginning of the paper for the reader's convenience.

II. Asynchronous Switch Design

The structure of the proposed LF-ASD is presented in Fig. 3. The design of the LF-ASD relies on a new feature basis derived from signal characteristics observed in the 1–4 Hz frequency band. The feature basis and feature selection process is reviewed in the next subsection. Details of the feature extraction methodology are given following the feature selection summary.

The LF-ASD feature classifier was implemented as a nearest neighbors ($k-NN$) classifier [10] because of its suitability with our small data sets. We selected a $1-NN$ for this

[1]Note, such a mechanism to determine intent is not required in synchronous control environments because the operator's intent to perform the control task is assumed at the beginning of the control period.

work.[2] To improve the speed of $1-NN$ classifier, a vector quantization technique, the LVQ3 algorithm [11] (with three codebook vectors per class), was applied to model the data set. LVQ3 has been used extensively in mu-power BCI techniques [12], [13]. The LF-ASD feature classifier performed a sample-by-sample classification of each feature vector generated by the feature extractor. The output of the state classification module is denoted by $z(n)$. The classification accuracy was found to improve when the $z(n)$ values were averaged over time.[3] We believe the reason for this improvement was because averaging emphasized temporally redundant information in neighboring $z(n)$ values, which were present because we oversampled the feature vector since we did not know the optimal classification rate for this new feature set. Thus, the output of the classifier, denoted $z_{ma}(n)$, is a moving average of $z(n)$ during a time period Δ. $z_{ma}(n)$ would be classified as control state C if more than l_o $z(n)$ values were classified as C, otherwise, as I. The optimal value for the parameter Δ was experimentally determined to be five; values greater than five did not provide any additional information [14].

Before we detail the feature extraction methodology used in the LF-ASD, we will provide some background on how the new feature basis was selected. Section II-A summarizes the findings of the preliminary studies used select a useful feature basis for asynchronous signal detection.

A. Feature Selection Overview

The purpose of the section is to present the feature basis used in the LF-ASD and illustrate how it was chosen. (For detailed methodologies and results from these studies, refer to [14]).

The initial objective of this work was to evaluate existing BCI feature sets to determine if these techniques were reasonable candidates for asynchronous switching. The OPM was considered first as it is the only BCI technique that has been designed specifically to differentiate idle from active (control) EEG in an asynchronous control application. However, our offline evaluations with this technique (detailed below) indicated limited ability. Although it had never been reported, mu-ERD [3], [6], the feature basis for state-of-the-art BCIs, seemed to be an excellent feature for asynchronous signal detection since it occurs when certain cognitive events are generated. However, our evaluation of an asynchronous switch based on mu-ERD feature classification demonstrated relatively high error rates when applied to this task. The details of this evaluation are given below. Given the relatively poor performance of existing techniques our focus changed to identify a new feature basis for asynchronous switching. Note, there are several other feature sets such as power spectral density coefficients (including beta rhythm power) [5], [9], or autoregressive parameters [7] that were not evaluated Their applicability to asynchronous control remains unknown.

Our search for an effective feature basis focused on imagined, voluntary movement-related potentials (VMRPs) because voluntary movement control is an existing, internal control system

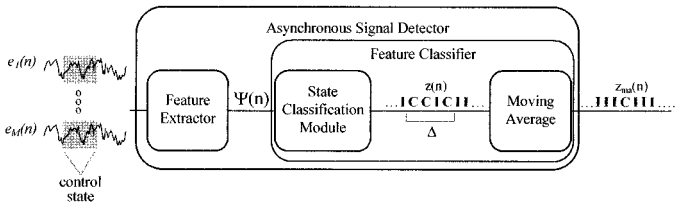

Fig. 3. Components of the ASD. $e_i(n)$ are the observed EEG signals at electrode pairs e_i, $i = 1, 2, \ldots, M$, and discrete time n. $\Psi(n)$ is the feature vector generated by the feature extractor. $z_{ma}(n)$ is the final classification sequence and the sequence, $z(n)$, is the sequence of sample-by-sample feature classifications. Note, I denotes an idle state classification and C denotes a control state classification.

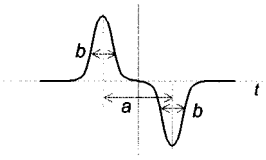

Fig. 4. Feature wavelet used for signal analysis during feature selection. Note, maximal elemental feature values were found for $b = 0$. With $b = 0$, the elemental features correspond to a difference in signal levels defined by (4).

in humans that seems naturally suited to drive a BCI. Other research laboratories have also taken this approach, using EEG features related to imagined movements as their basis for control [13], [15].

However, signal analysis of imagined movements in asynchronous control environments is difficult because one needs an indication of intent in order to process the data. This is not the case for synchronous applications because user intent is assumed during the control periods. The only method to record intent for imagined movements in asynchronous control environments is for subjects to self-report intent during the data recording. There are two disadvantages to self-reporting. The first is that self-report complicates the signal analysis because one does not know exactly when the movement was made. The second problem is that it is hard to provide the user with any form of feedback during these sessions. In order to avoid these problems at this initial stage of development and evaluation of our switch prototype, we chose to analyze VMRPs under the assumption that features discovered for VMRPs would be applicable to imagined movements. This assumption has support in the findings of Cunningham *et al.* [16] who observed that although the late MRP component over the primary cortex was reduced in amplitude during imagined movements compared with actual movements, the early MRP components did not differ in amplitude or temporal and topographic characteristics.

Time-frequency analysis [17] of attentive idle and movement-related EEG indicated a noticeable relative power increase in the 1–4 Hz band in ensemble data over five subjects. Our initial research into the 1–4 Hz range used a classifier designed to discriminate single-trial idle and movement EEG using 1–4 Hz power levels. However, this classifier did not perform better than chance [14].

Analysis of the 1–4 Hz frequency band with the bi-scale wavelet,[4] $w(\boldsymbol{a},\boldsymbol{b})$, shown in Fig. 4, exposed a set of relatively

[2]Other implementations of $(k-NN)$ may prove to be optimal, but these were not evaluated.

[3]Anderson, *et al.* [7] have also observed that temporal averaging can improve classification performance.

[4]This wavelet shape was selected to respond to the RP-PMP-MP transitions known to exist in 1–4 Hz, ensemble-averaged VMRPs.

stable features over the supplementary motor area (SMA) and primary motor area (MI). Mathematically these wavelet features were defined as

$$E(n, k, \boldsymbol{a}, \boldsymbol{b}) = \sum_{n=-\infty}^{\infty} w(\boldsymbol{a}, \boldsymbol{b}) \cdot e_k(n) \tag{1}$$

where $e_k(n)$ is the kth observed bipolar EEG signal (filtered to 1–4 Hz using a 121-point, zero-phase finite impulse response filter based on a Hamming window).

The discriminatory power of several elemental features of the form

$$E_i(n) = E(n, k_i, a_i, b_i) \tag{2}$$

was evaluated on the attentive idle and movement-related EEG. We found it useful to introduce a time shift, d_i, to each elemental feature to allow for the phase alignment of features. Also, we noticed that the strongest feature values were observed for the b_i parameters near zero, so we simplified our analysis to $b_i = 0$, for all i. These actions reduced the feature wavelet to a difference of impulses and reduced the complexity of elemental features to

$$E_i(n) = E(n - d_i, k_i, a_i, 0) \qquad i = 1, 2, \ldots, M \tag{3}$$

where M indicates the number of features evaluated. (3) can be rewritten as

$$E_i(n) = e_{k_i}(n + \alpha_i) - e_{k_i}(n + \beta_i) \tag{4}$$

to express the features in terms of the recorded signals. In this form, the signal delay parameters are defined as

$$\alpha_i = d_i - a_i/2 \quad \beta_i = d_i + a_i/2. \tag{5}$$

The robustness of the feature prediction was improved by pairing elemental features in compound features defined by the correlation

$$\begin{aligned} g_{ij}(n) &= E_i(n) \cdot E_j(n), \qquad \text{if } E_i(n) \geq 0 \text{and } E_j(n) \geq 0 \\ &= 0, \qquad \text{otherwise.} \end{aligned} \tag{6}$$

Note, the $g_{ij}(n)$ feature values were set to zero if either $E_i(n)$ or $E_j(n)$ were negative, to avoid generating large feature values from negative images of the desired phasic relationships.

Many compound features were evaluated on signals measured between electrodes AF_z, F_1, F_z, F_2, FC_3, FC_1, FC_3, FC_2, FC_4, C_3, C_1, C_3, C_2, C_4, P_z, and O_z in the International 10–20 System for electrode placement. The features were ranked based on the difference of the median feature values between active and idle training sets.

The strongest discriminatory features were found in autocorrelations within six electrode pairs F_1–FC_1, F_z–FC_z, F_2–FC_2, FC_1–C_1, FC_z–C_z and FC_2–C_2 [14]. These six compound features, which had difference of medians values in the range 161–183 units, were the features chosen for the evaluation of our asynchronous switch prototype (described below). Some of the other features displayed nearly as strong discrimination power (e.g., the seventh strongest feature, within the electrode pair FC_1-FC_z, had a difference of medians value of 153 units).

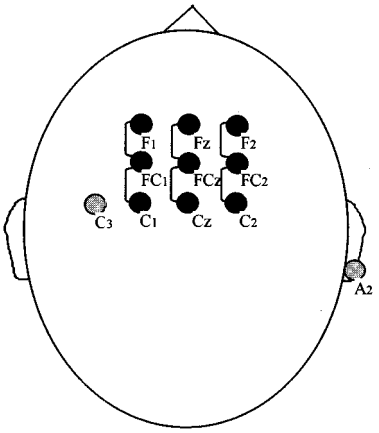

Fig. 5. Electrode placement for LF-ASD.

We chose to limit the features to the top six primarily because these features were the minimal set that provided uniform coverage of the motor areas of the cortex. Since these features were related to VMRP amplitude peaks, which have been shown to be relatively consistent between subjects and stable over time [18]–[21], we assumed that these features would be stable and generally applicable.

As a summary note, Birbaumer *et al.* has recently reported a technique that also uses low-frequency features recorded from the frontal cortex [22], but their feature set is not related to ours. Their technique is based on a completely different neurological mechanism, slow cortical potentials, where ours is based on imagined movement-related potentials.

B. Feature Extraction Methodology

Six signals were recorded from the six electrode pairs shown in Fig. 5 using a sample rate of 64 Hz. These signals were prefiltered between 1 and 4 Hz and the compound features described by (6) were calculated. The delay parameters [defined in (5)] were selected from an exhaustive parametric search through training data. Note that during feature selection, the feature delay values for common electrode pairs (e.g., F_i–FC_i) were constrained to be equal (as seen in Table I).[5] In order to increase the robustness of the signal detection to trial-by-trial latency variation, the feature values given by (6) were collapsed over 1/8 of a second into the aggregate features defined by

$$G_{ij}(n) = \max(g_{ij}(n-8), g_{ij}(n-7), \ldots, g_{ij}(n+7)) \tag{7}$$

where $\max()$ represents the maximum. The resulting feature vector, $\Psi(n)$, was an equally weighted, six-dimensional vector, with each dimension reflecting the value of an aggregate feature.

III. LF-ASD Evaluation Methodology

The purpose of the offline study was to determine how well the LF-ASD could discriminate EEG activity related to imag-

[5]The original aim of this constraint was to generalize the design of the LF-ASD to all types of movements instead of optimizing it for a right index finger flexion. This constraint is unnecessary for the LF-ASD as presented but is described because the performance was evaluated with this constraint applied. We plan to remove it in future work.

ined movements from attentive idle EEG. However, we needed an experimental design that would indicate the subjects' intent to operate the asynchronous switch during imagined movements. As with our signal analysis, we chose to use the mental state related to an actual movement to approximate the mental state related to an imagined movement. This choice allowed us to have accurate time stamps on subject intent and it allowed us to provide reliable feedback to the subjects during recording. Of course, this approach relies on our assumption that the imagined movements will have enough similarity to actual movements to drive the LF-ASD.

To evaluate the new feature set, the LF-ASD design, described in Section II, was used with the single set of delay parameters. A single set of delay parameter was selected to limit the complexity of this initial evaluation of our prototype. We believed that parameters estimated from a data set with the strongest VMRPs would provide our best results across all subjects. With this belief, the delay parameters for this study were determined from Subject 3's training data, because this subject's data set had the largest ensemble-averaged VMRP response of the five subjects. The selected delay parameters are shown in Table I. (These six compound features were labeled $f_l, l = 1, 2, \ldots, 6$ to simplify the discussions in the following sections.)

The performance of the LF-ASD was contrasted to two other ASDs: one based on mu-power features and another based on the OPM algorithm.

The second asynchronous switch in this evaluation, referred to as Mu-ASD, implemented mu-rhythm power feature extraction and classification on a signal measured from a monopolar electrode at C_3 similar to the implementation described in [6]. Notable differences in implementation were the reference mu power level used for discrimination, subject training, and temporal averaging of output classifications. For this study, the average power over the first second of each 4-s experimental trial (defined below), which was known to be the idle state, was assumed to be a reasonable reference mu power level. We did not have the means to train subjects in a manner similar to [6], but we felt that an evaluation based on untrained subjects would not be a fair comparison and it would be too easily criticized. So for .5 s before and after all experimental finger flexions (defined below), the recorded power in the 8–12 Hz band was artificially reduced to twice the power in the 18–22 Hz band to approximate the effect of subject training. This scaling was based on the observation that mu-power levels for trained subjects seemed to be approximately twice the power in the 18–22 Hz band [3], [23]. The State Classification Module for Mu-ASD was selected as a $1-NN$ classifier with the feature space modeled by the LVQ3 algorithm with three codebook vectors per class [11]. Like the LF-ASD, the classifier output was fed through a moving average module in order to facilitate the comparison with the LF-ASD performance.

The third asynchronous switch, referred to as OPM-ASD, implemented the OPM algorithm as described by Birch *et al.* [1] with two exceptions: Shorter (1 s) segments were classified every 1/16 of a second and the classifier output was fed through a moving average module in order to facilitate the comparison with the Mu-ASD and LF-ASD performance. The shorter segments were necessary to match the asynchronous classification rates tested on the other ASDs. To summarize the original OPM method, a one-dimensional EEG signal related to an imagined voluntary movement is recorded from monopolar electrode at C_3. This signal is assumed to be composed of an imagined movement-related potential (the signal of interest) added to spontaneous EEG (considered background noise). The method attempts to estimate the spontaneous EEG component, then subtract it from the original signal to yield the signal of interest. The estimated imagined movement-related potential is then classified using a linear classifier based on time-warping. In order to estimate the spontaneous EEG from the input signal, the OPM uses robust statistical processing algorithms. For more details of this technique, refer to [1].

TABLE I
OPTIMAL 1–4 HZ FEATURES. FOR A DEFINITION OF THE SYMBOLS REFER TO (1), (4)–(6)

	$E_i(n)$			$E_j(n)$		
	$e_{k_i}(n)$	α_I *	β_i *	$e_{k_j}(n)$	α_j *	β_j *
f_1	F_1-FC_1	-1	+25	F_1-FC_1	0	+50
f_2	F_z-FC_z	-1	+25	F_z-FC_z	0	+50
f_3	F_2-FC_2	-1	+25	F_2-FC_2	0	+50
f_4	FC_1-C_1	-1	+15	FC_1-C_1	-12	+30
f_5	FC_z-C_z	-1	+15	FC_z-C_z	-12	+30
f_6	FC_2-C_2	-1	+15	FC_2-C_2	-12	+30

*Units for delay parameters are (discrete time) samples.

Table II summarizes the makeup of each of the experimental ASDs.

For all the ASDs, a decision rate of 16 decisions/s was chosen. This relatively high decision rate was a conservative choice, known to be faster than EEG state changes related to a movement and twice that used in a mu-power classifier [6].

The performance of these ASDs was evaluated in terms of the probabilities of true and false positives $[P(TP)$ and $P(FP)]$ relative to a movement event.

A. Data Collection

Data was collected from five, right-handed males within the age range of 23–33. All the subjects in this experiment were strongly right-hand dominant as measured by handedness scores from the LAT-24-R questionnaire.[6] Each subject participated in a single 3-hour recording period and the five subjects were recorded on separate days over a period of a month.

The subjects were seated in a comfortable chair with their eyes 100 cm from the visual display. Each subject wore an ElectroCap electrode cap with signals measured from the locations shown in Fig. 5. EOG activity was measured above and to the left of the left eye.

[6]The LAT-24-R handedness Inventory was supplied and rated by the Human Neurophysiology and Perception Laboratory at the University of British Columbia, Vancouver, BC, Canada.

TABLE II
DEFINITION OF ASYNCHRONOUS SWITCH DESIGNS USED IN EVALUATIONS. REFER TO THE TEXT FOR DESCRIPTIONS OF SYMBOLS

Switch Design	Feature Extractor	Feature Classifier	
	Output, $\Psi(n)$	Classification Method	Feature Space Modeling
LF-ASD	$[f_1(n), f_2(n), f_3(n), f_4(n), f_5(n), f_6(n)]$	1-NN	LVQ3
Mu-ASD	estimated mu power relative to reference power	1-NN	LVQ3
OPM-ASD	cost of time-warped VMRP estimate from OPM	linear classifier	none

The subject wore a custom data glove with two piezo-electric sensors located over the metacarpal-phalanges joint and the phalanges-phalanges joint of the right index finger [14]. The glove produces a signal that depended on the degree and speed of a right index finger flexion. The finger position signal was also recorded by the data acquisition system.

The EOG and EEG signals were amplified by a Biomedical Monitoring Systems Inc. EEG system and recorded with the finger movement on the data acquisition system consisting of an IBM compatible computer with a Data Translation 2801A digital-to-analog board and running IMPULSE EEG Data Collection software. Signals were recorded at 128 Hz, but downsampled to 64 Hz prior to evaluation.

The desired movement was explained to the subject and the subject was allowed to practice while the investigator watched and corrected the subject's motion. A nonstandard finger flexion was selected as the target movement because it was assumed to be new to all subjects. Pilot studies showed that this movement required attention and a moderate amount of effort to perform accurately. The selected movement was a fast (less than 1 s), compound, index finger flexion. The movement started with the flexion of the index finger at the metacarpal-phalanges joint, followed immediately by a ballistic palmar flexion of the index finger. The investigator used visual inspection of averaged finger movements to maintain similar movement patterns between subjects. After training and instruction, the subject was allowed to practice at the experimental sequence until at least ten movements were attempted and greater than six out of ten movements were recognized by the system in ten consecutive trials.

An experimental control system, referred to as MONITOR, controlled the video display and evaluated EOG and finger movement quality. The data acquisition system would receive signals from MONITOR when a trial started and when a finger movement was detected, enabling the recorded EEG to be time stamped for these events. To evaluate finger movement quality, MONITOR performed a weighted-correlation comparison of each movement against a subject-specific movement template that was recorded at the start of the experiment.

Throughout the experiment, the subject focused on a "pong" style video display similar to the one shown in Fig. 6. This display was introduced in an attempt to increase subject attention and decrease eye fatigue.[7] The monochrome monitor displayed two balls moving within a rectangular boundary at a moderate speed of approximately 4 cm/s The center ball moved through a visual angle of 2° up and down or side to side. The second ball, marked 2 in Fig. 6, moved randomly throughout the space bouncing off the boundary and the center ball. The 4×6 cm boundary, labeled as 3 in Fig. 6, was either a single-lined or a double-lined rectangle.

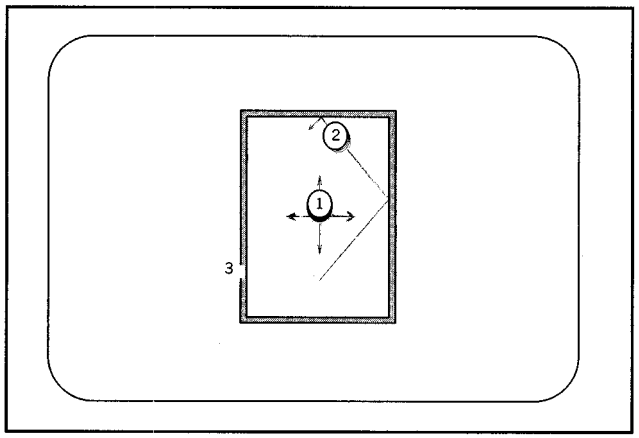

Fig. 6. Experimental display.

The system was configured so that the direction of the center ball movement was changed from vertical to horizontal 1 s after the subject flexed his finger. The 1-s delay was necessary to eliminate the possibility of a visual evoked potential in the recorded data caused by the orientation change.

The subject was instructed to pay attention to the boundary box. When the single-line boundary box was displayed, the subject was instructed not to move, but to keep monitoring for possible collisions between the outer and center ball. During this time, the MONITOR system would attempt to locate a 4-s period free of EOG and movement artifact. When it successfully found such a period, the 4-s period was recorded as an attentive idle trial.

[7]Studies to evaluate the effects of this display were conducted on each subject. Each subject's EOG was visually inspected and found to be the same regardless of whether they kept their eyes on the center ball, the outer ball, or fixed on a corner of the display box.

When the boundary box on the video display changed from a single line to a double line, the subject was instructed to wait for at least 3 s and then make a movement. The decision of when to move was left to the subject. Sufficient practice was allowed so the subject had a sense for the 3-s delay without having to mentally count the time. The subject was instructed to try to time their movements in order to position the center ball in the path of the outer ball. If the subject moved before 3 s had elapsed, a message "too soon" appeared on the screen for 2 s. After the subject moved, the direction of the center ball changed from vertical to horizontal (or visa versa) 1 s after the movement. If the subject reproduced the trained movement, the center ball would flash rapidly on and off (after a 1-s delay) for 500 ms indicating a successful reproduction. The primary task, as explained to the subjects, was to try to make the center ball flash by reproducing the trained movement. If the movement correlated with the system template with a value greater than 0.9 and there was no EOG contamination for 3 s prior to and 1 s after the start of the movement, the EEG at that point was marked as a successful ("good") movement.

The subject was instructed not to worry about blinking, but to keep their eyes open for as long as they comfortably could. It was stressed that there was no penalty for blinking and it was more important for the subject to blink if he felt he needed to do so.

During the experiment the subject performed a series of active and idle tasks in a random order selected by the MONITOR system at run time. The MONITOR system was programmed to ignore the first ten active and first ten idle trials (good or bad) to avoid start-up effects. Data collection continued until 50 successful movements and 50 attentive idle trials were recorded. Within MONITOR, the system was programmed to wait up to 20 s for a movement before aborting and going on to the next state. The idle state was programmed to wait for, at most, 12 s before going to the next state with a maximum of two idle states shown in a row. These presentation criteria were determined from pilot studies to be optimal for collecting a 4-s period of artifact-free idle EEG while not increasing eye fatigue and loss of attention due to long periods of inactivity.

Every 8 min, or when the subject requested or appeared to need a break (as indicated by excessive blinking or consistently poor movement performance), a break was taken. The experiment was resumed at the subject's convenience and comfort.

IV. Results

The performance of the ASDs to discriminate between attentive idle EEG and movement-related EEG was evaluated offline. The results are summarized in the Receiver Operating Characteristic Curves (ROCC) shown in Figs. 7–9. Note that confidence intervals were excluded from the ROCCs to improve clarity. For all these points, the standard deviation of the $P(TP)$ estimates was between 5% and 12% and the standard deviation of the $P(FP)$ estimates was between 2% and 3%.

For the reader who is not familiar with ROCCs, the ROCCs capture an application-independent representation of expected operating characteristics in terms of the probability of true positives (movement-related EEG being classified as movement-related EEG) and probability of false positives (attentive idle EEG being classified as movement-related EEG) [24].

In this study, the $P(TP)$ and $P(FP)$ values were calculated empirically. The $P(TP)$ and $P(FP)$ values were calculated from switch evaluations using a ninefold cross-validation pro-

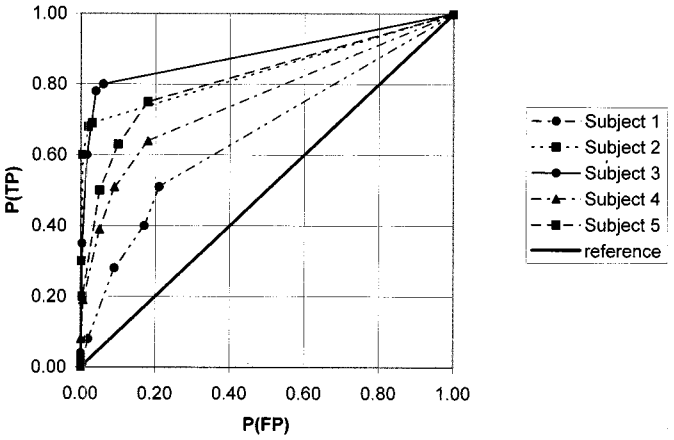

Fig. 7. ROCC of the LF-ASD signal detector when connected to Subjects 1 to 5.

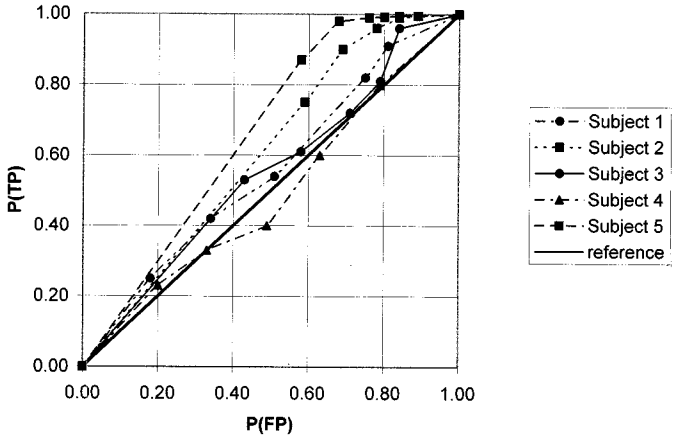

Fig. 8. ROCC of the Mu-ASD signal detector when connected to Subjects 1 to 5.

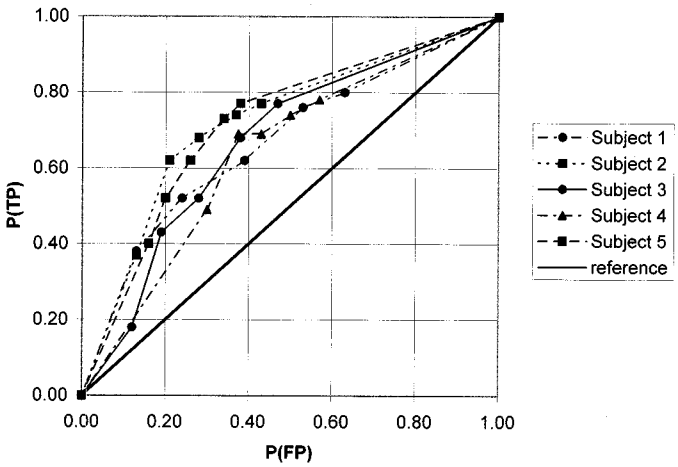

Fig. 9. ROCC of the OPM-ASD signal detector when connected to Subjects 1 to 5.

TABLE III
MEAN AREA UNDER THE ROC CURVE FOR THE ROC CURVES SHOWN IN FIGS. 7–9

	Subject 1	Subject 2	Subject 3	Subject 4	Subject 5
LF-ASD	0.66	0.84	0.89	0.76	0.82
Mu-ASD	0.55	0.61	0.55	0.49	0.66
OPM-ASD	0.66	0.72	0.67	0.64	0.72

cedure. In this procedure, 90 randomly selected active and idle trials (45 of each) were divided into nine equal subgroups of five active and five idle trials. Sequentially, one subgroup was removed and the remaining 40 active and 40 idle trials were used to train the feature detectors. The subset of trials left out of the construction of each feature detector was used by the corresponding feature detector to generate ten unbiased $z(n)$ sequences (5 from active trials and five from idle trials). All incorrect classifications during an idle trial [i.e., any $\boldsymbol{C}$ classification in $z_{ma}(n)$] were considered false positives. Since each idle trial had 53 classifications over the 3.5-s period, each trial could produce from zero to 53 false positives. For active trials, a $\boldsymbol{C}$ classification at the trigger point was considered a true positive. The classifications during the other parts of the active trial were not included in the reported probabilities.[8] In total, 90 $z(n)$ sequences were generated for each ASD using this approach. The average $P(TP)$ and $P(FP)$ and the standard deviation of these estimates were calculated from these 90 sequences. For the relatively small active data set, estimates of the mean and variance of $P(FP)$ were calculated using the standard estimates for proportions. Estimates for the mean and variance of $P(FP)$ were calculated using standard formulas for random variables.

In order to compare error rates of these ASDs, the area under the ROCC is often used as an overall indication of the system's performance abilities. For a two-choice decision problem (like the one studied here), the mean Area Under the ROC Curve is a measure of the mean percent correct classifications of the receiver. We have summarized the mean Area Under the ROC Curves in Table III for all subjects and ASD techniques.

As seen in the values of Table III, the mean Area Under the ROC Curve (i.e., the mean percent of correct classifications) was 10%–22% larger than the area of the OPM-ASD for all subjects, except Subject 1 (where the area was equal). In the case of the Mu-ASD, the mean Area Under the ROC curves portrayed a weak ability to discriminate.

The estimated mean error rate and the mean cost of an error for a specific application can be derived from points on the ROCCs. For example, the estimated mean error for an application can be estimated from any point on these curves using

$$P(E, \lambda) = \lambda \cdot (1 - P(TP)) + (1 - \lambda) \cdot P(FP) \quad (8)$$

[8]This approach for measuring true positives was selected because the trigger point was the only point where we were sure of the subjects' intent to move. Preliminary analysis of the classifications around the movement [16] suggests that the periods within 1 s around the movement contain information that may be used to improve the classification accuracy. However, we did not want to bias the $P(TP)$ rate in this study with classifications that may be associated with the intended movement. How to exploit this information in an on-line implementation of the LF-ASD remains to be determined

where λ is the expected control state probability, P(control state). In the results described below, a z test statistic was used to compare the estimated mean error rates of the LF-ASD, OPM-ASD and Mu-ASD for various values of λ.

The minimum mean probability of error for each ASD was calculated from (8) for various values of λ. The minimum mean probability of error of the LF-ASD was shown to be significantly lower ($p <= 0.001$, with $\lambda \leq 0.2$ and $p <= 0.05$ with $\lambda \leq 0.5$) than the mean minimum probability of error for both Mu-ASD and OPM-ASD for all subjects.

The low-frequency asynchronous signal detector (LF-ASD), which was based on the 1–4 Hz feature set, was able to differentiate index finger flexions from attentive idle EEG with error rates significantly better than chance. For example, the LF-ASD was able to achieve $P(TP)$ values in the range of 60%–81% with corresponding $P(FP)$ values in the range of 1.6%–6.0% when classifying Subject 3's data. Although the feature delay parameters were calibrated using Subject 3's training data, the LF-ASD was able to achieve $P(TP)$ in the range of 38%–76% corresponding to $P(FP)$ values in the range of 0.3%–18% for all other subjects (excluding Subject 1).

Subject 1 performed the worst with $P(TP) < 40\%$ and the $P(FP) > 16\%$, which was consistent with the observation that his data had the weakest ensemble averages of all the subjects. The reader should note that Subject 1 was an advanced classical guitarist and that the movement was very much like the plucking of a guitar string. The issue of whether his guitar training influenced the size of his VMRPs was recognized but was not resolved.

The proposed LF-ASD is considered to be relatively stable over time and across subjects although this property has not been extensively tested. The support for this view comes from several observations. First, the LF-ASD was based on amplitude and phase relationships between the dominant peaks present in ensemble averages. These features are known to be stable over time for a subject [18]–[21]. Second, the trial-by-trial detection performance of the 1–4 Hz feature set did not vary over the 3-hour data-recording period for each subject. Third, the LF-ASD for all the subjects performed with error rates significantly better than chance with the LF-ASD calibrated for Subject 3. This result implies that the subjects share a base set of features. Since the data for the subjects were recorded on separate days over a period of a month, this base set of low-frequency features appears to be stable in time.

Less than 30% of the idle trials for each subject were found to contain the majority of the idle activity that was classified as false positives. This indicates that the LF-ASD could correctly classify relatively long periods of idle EEG (at least 3.5 s long)

without any false positives. Further analysis is required to determine if the idle trials that contained the majority of the false positives actually contained a special type of idle activity distinguishable from movement-related EEG.

Trials recorded for the same movement were found to contain VMRPs of varying peak amplitude. Trials with the "weaker" VMRPs were suspected of biasing the performance results. By removing 10% of the trials with the "weakest" VMRP amplitude, the reported $P(TP)$ rate increased by 10%–20%. Preliminary follow-up studies [25] have shown that subject training can increase the consistency of the VMRPs and feature strength during the control state and as a result, increase the $P(TP)$.

The results of ASD performance evaluation demonstrated that both the OPM and mu-ERD classification techniques produced significantly higher mean error rates than the LF-ASD. The OPM-ASD generated moderately high $P(FP)$ values for corresponding $P(TP)$ values (e.g., $P(FP)$ values in the range of 25%–35% for corresponding $P(TP)$ values in the range of 49%–74%). The minimum mean error rates for the OPM-ASD were significantly higher ($p <= 0.001$ for $\lambda <= 0.2$; $p <= 0.05$ for $0.2 < \lambda <= 0.5$) than the minimum mean error rates of the LF-ASD across all subjects. Although the $P(TP)$ values for OPM-ASD (67%) were similar to those reported by Birch [1], the $P(FP)$ values were dramatically larger (30% versus 3%). Three possible explanations are offered for this discrepancy. First, this study used ballistic finger flexions, which have a shorter and weaker VMRP than the skilled thumb movement used by Birch. The OPM algorithm therefore may have had a harder time extracting an estimate of this VMRP. The second reason was Birch only performed one classification per idle trial with a relatively long (4 s) template. That resulted in an artificially low estimate of $P(FP)$. In contrast, this study evaluated the OPM algorithm every 1/8 s with a shorter (1 s) template which would be required in a responsive BCI. Finally, this study compared attentive idle EEG in contrast to the nonattentive idle EEG used by Birch. This difference in attention control implies that the original results reported for OPM may have relied on the shifts in attention level to aid its classification.

As identified in the Section II, mu-power measures seemed naturally suited for an ASD, but this functionality has not been demonstrated. The results reported above demonstrated that our implementation of mu power was not a good method for discriminating index finger flexions from attentive idle EEG. The Mu-ASD generated relatively high $P(FP)$ values for corresponding $P(TP)$ values. The minimum mean error rates for the Mu-ASD were significantly higher ($p <= 0.001$ for $\lambda <= 0.5$) than the minimum mean error rates of the LF-ASD across all subjects. We noticed that the attentive idle EEG had frequent power fluctuations in the mu band and we suspect the Mu-ASD could not distinguish these from the mu-power level during movement. This may explain its poor performance.

V. Discussion

This paper has focused on an important class of applications for BCI application: asynchronous control applications. We have distinguished these types of applications from synchronous control applications and have emphasized the main problems related to the measurement of user intent. This work provides the first extensive evaluation of an asynchronous signal detection device in attentive spontaneous EEG.

We have presented a prototype of an asynchronous switch, the LF-ASD, which we believe will be suitable for asynchronous BCI control applications. This switch design is based on a methodology to recognize a unique set of signal features identified in the 1–4Hz band. The prototype switch design has demonstrated a strong potential for recognizing single-trial VMRPs. For reasons given previously, we assume that these features will work for imaginary movements, but this assumption remains to be verified. The introduction of the LF-ASD is our first step toward a critical class of component for asynchronous control applications.

The primary objective in our offline evaluation of the LF-ASD was to demonstrate the discriminatory power of our new 1–4Hz feature set. In our offline studies, the LF-ASD functioned with classification error rates significantly better than chance. For instance, the LF-ASD achieved $P(TP)$ values in the range of 38%–78% corresponded to $P(FP)$ values in the range of 0.3%–11.6% for four out of five subjects. With the best subject, $P(TP)$ values in the range of 60%–81% corresponded to $P(FP)$ values in the range of 1.6%–6.0%. We expect improvements to this initial design will lead to improved performance. The new feature set requires minimal computation to calculate, which means that the LF-ASD can be implemented in a real-time with current technology.

The results of our evaluations of asynchronous switches based on the OPM and mu-ERD feature sets suggest that neither of these methods as implemented is well suited for asynchronous control. Given the number of configurable parameters, there may exist alternate implementations of OPM or mu-ERD (or other feature sets such as Beta rhythm power, power spectral density coefficients, or autoregressive parameters) that may prove useful.

A. Future Work

The focus of the reported work was to verify that the 1–4Hz feature basis had sufficient power to discriminate VMRP and attentive idle activity. Our current research is focused on verifying the LF-ASD operation online with real and imaginary movements with able-bodied subjects and people with severe motor disabilities. This work involves exploring methodologies to capture users' intent with imagined movements. A preliminary follow-up study of an online LF-ASD implementation [25] has confirmed the base error rates reported here and it has shown that individuals can improve their ability to use the LF-ASD through training.

Many boundary characteristics such as maximum switch operating speed also remain to be quantified.

We are also interested in subject training (how well can the subject adapt to the LF-ASD) and how well the LF-ASD can be customized to an operator. As a preliminary test in this area we customized the LF-ASD feature delay parameters to Subject 4;

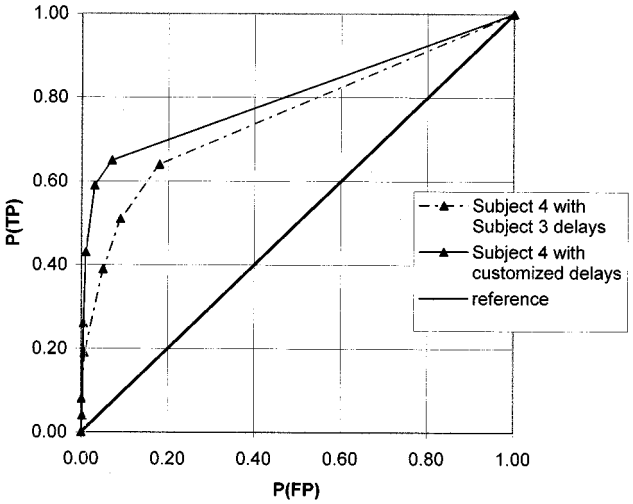

Fig. 10. ROCC illustrating improved operating characteristics with LF-ASD delay parameters customized for Subject 4.

previously these parameters were calibrated to Subject 3. The increase in performance is shown in Fig. 10; the area between the operating curve and the reference line increased by 18%.

Future work will also attempt to improve the LF-ASD design, possibly generalizing it to a variety of movements, thus, making it an asynchronous, multiposition switch. We are also considering the use of the proposed asynchronous switch as a front end for other BCI techniques that have been developed for synchronous application environments. In this type of compound system, the user could operate the LF-ASD to initiate the control period for another BCI controller.

REFERENCES

[1] G. E. Birch, P. D. Lawrence, and R. D. Hare, "Single trial processing of event related potentials using Outlier information," *IEEE Trans. Biomed. Eng.*, vol. 40, no. 1, pp. 59–73, Jan 1993.

[2] S. G. Mason, G. E. Birch, and M. R. Ito, "Improved single-trial signal extraction of low SNR events," *IEEE Trans. Signal Processing*, vol. 2, pp. 423–426, Feb. 1994.

[3] J. R. Wolpaw, D. McFarland, G. W. Neat, and C. A. Forneris, "An EEG-based brain-computer interface for cursor control," *Electroencephalogr. Clin. Neurophysiol.*, vol. 70, pp. 710–523, 1991.

[4] S. Bozinovski, M. Sestokov, and L. Bozinovska, "Using EEG alpha rhythm to control a mobile robot," in *Proc. Annu. Int. Conf. IEEE Engineering in Medicine and Biology Society*, 1989.

[5] Z. A. Keirn and J. I. Aunon, "A new mode of communications between man and his surroundings," *IEEE Trans. Biomed. Eng.*, vol. 37, pp. 1209–1214, Dec. 1990.

[6] G. Pfurtscheller, D. Flotzinger, and J. Kalcher, "Brain-computer interface—A new communication device for handicapped persons," *J. Microcomput. Applicat.*, vol. 16, pp. 293–299, 1993.

[7] C. W. Andersen, E. A. Stolz, and S. Shamsunder, "Multivariate autoregressive models for classification of spontanesous electroencephalographic signals during mental tasks," *IEEE Trans. Biomed. Eng.*, vol. 45, Mar. 1998.

[8] T. M. Vaughan, J. R. Wolpaw, and E. Donchin, "EEG-based communication: Prospects and problems," *IEEE Trans. Rehab. Eng.*, vol. 4, pp. 425–430, Apr. 1996.

[9] J. Kalcher, D. Flotzinger, C. Neuper, S. Golly, and G. Pfurtscheller, "Graz brain-computer interface II: Toward communication between humans and computers based on online classification of three different EEG patterns," *Med. Biol. Eng. Comput.*, vol. 34, no. 5, pp. 382–388, 1996.

[10] C. W. Therrien, *Decision Estimation and Classification*. New York: Wiley, 1989.

[11] T. Kohonen, "The self-organizing map," *Proc. IEEE*, vol. 78, pp. 1464–1480, Sept. 1990.

[12] D. Flotzinger, J. Kalcher, J. R. Wolpaw, D. McFarland, and G. Pfurtscheller, "Off-line classification of EEG from the New York brain-computer interface (BCI)," Institute for Information Processing, Graz, Austria, Tech. Rep. 378, 1993.

[13] G. Pfurtscheller, C. Neuper, and D. Flotzinger, "EEG-based discrimination between imagination of right and left hand movement," *Electroencephalogr. Clin. Neurophysiol.*, vol. 103, pp. 642–651, 1997.

[14] S. G. Mason, "Detection of single-trial index finger flexions from continuous, spatiotemporal EEG," Ph.D. dissertation, Univ British Columbia, Vancouver, Canada, 1997.

[15] W. D. Penny, S. J. Roberts, and M. J. Stokes, "Imagined hand movements identified from the EEG mu-rhythm," *J. Neurosci. Meth.*, 1998.

[16] R. Cunningham, R. Iansek, and J. L. Bradshaw, "Movement-related potentials associated with movement preparation and motor imagery," *Exp. Brain Res.*, vol. 111, pp. 429–436, 1996.

[17] H. I. Choi, W. J. Williams, and H. Zaveri, "Analysis of event related potentials time-frequency energy distribution," in *Proc. 24th Annu. Rocky Mountain Bioengineering Symp.—Biomedical Sciences Instrumentation Instrument Society of America*, 1987.

[18] L. Deecke, P. Scheid, and H. Kornhuber, "Distribution of readiness potential, pre-motion positivity and motor potential of the human cerebral cortex preceding voluntary finger movements," *Exp. Brain Res.*, vol. 7, pp. 158–168, 1969.

[19] C. H. M. Brunia, "Movement and stimulus preceding negativity," *Bio. Pysch.*, vol. 26, pp. 165–178, 1988.

[20] H. G. Vaughan Jr. and L. D. Costa, "Topography of the human motor potential," *Electroencephalogr. Clin. Neurophysiol.*, vol. 25, pp. 1–10, 1968.

[21] G. Goldberg, "Supplementary motor area structure and function: Review and hypotheses," *Behavioral Brain Sci.*, vol. 8, pp. 567–616, 1985.

[22] N. Birbaumer, N. Ghanayim, T. Hinterberger, I. Iversen, B. Kotchoubey, A. Kuebler, J. Perelmouter, E. Taub, and H. Flor, "A brain-controlled spelling device for the completely paralyzed," *Nature*, vol. 398, pp. 297–298, 1999.

[23] M. J. Foster, D. McFarland, and J. R. Wolpaw, "Improvement in EEG-based brain-computer communication by use of additional recording locations," in *Proc. RESNA '95 Annu. Conf.*, Vancouver, Canada, 1995, pp. 687–689.

[24] D. M. Green and J. A. Swets, *Signal Detection Theory and Psychophysics*. New York: Wiley, 1966.

[25] D. Lisogurski and G. E. Birch, "Identification of finger flexions from continuous EEG as a brain computer interface," in *Proc. IEEE Engineering in Medicine and Biology Society 20th Annu. Int. Conf.*, Hong Kong, 1998.

Steven Mason (S'91–M'98) received the B.E.Sc. degree in electrical engineering and B.Sc. in computer science from the University of Western Ontario, London, ON, Canada, in 1987 and the M.A.Sc. and Ph.D. degrees in electrical engineering (biomedical signal processing) from the University of British Columbia, Vancouver, Canada, in 1991 and 1997, respectively.

He is currently leading the Brain-Computer Research Project for the Neil Squire Foundation in Vancouver, Canada. His research interests include human-machine interface design, statistical signal processing, biometric transducers for affective computing, embedded-systems design, and advanced interface techniques for interactive art, music, and dance.

Gary Birch (S'81–M'88) received the B.A. Sc. degree in electrical engineering, and the Ph.D. degree in electrical engineering (biomedical signal processing), both from the University of British Columbia, Vancouver, BC, Canada, in 1983 and 1988, respectively.

He was appointed Director of Research and Development at the Neil Squire Foundation, Vancouver, Canada, in August 1988 and then in May 1994 was appointed Executive Director. He is responsible for the on-going operations at the Neil Squire Foundation including the supervision of a Research and Development team; the preparation of contract proposals and budgets for government sponsored service delivery, and research and development projects; negotiating collaborative research and development projects with private sector companies, the future direction and development of the Neil Squire Foundation and is involved in the process of transferring research and development projects ready for commercial manufacturing. His recent and current professional contributions are: Adjunct Professor at UBC, Department of Electrical Engineering since July 1989; Adjunct Professor, SFU, Gerontology Research Program since July 1990; Member of the Minister's National Advisory Committee for Industry Canada on Assistive Devices since 1996; Member of the Executive Technical Committee on Assistive Technologies for Persons with Disabilities for the Canadian Standards Association since 1996; Member of the Premier's Advisory Council on Science and Technology since 1993. His specific areas of expertise are robotic control systems, EEG signal processing, digital signal processing, human-machine interface systems, and biological systems.